We are IntechOpen, the world's leading publisher of Open Access books Built by scientists, for scientists

6,900
Open access books available

185,000
International authors and editors

200M
Downloads

Our authors are among the

154
Countries delivered to

TOP 1%
most cited scientists

12.2%
Contributors from top 500 universities

WEB OF SCIENCE™

Selection of our books indexed in the Book Citation Index in Web of Science™ Core Collection (BKCI)

Interested in publishing with us?
Contact book.department@intechopen.com

Numbers displayed above are based on latest data collected.
For more information visit www.intechopen.com

12

ICA Applied to VSD Imaging of Invertebrate Neuronal Networks

Evan S. Hill[1], Angela M. Bruno[1,2], Sunil K. Vasireddi[1] and William N. Frost[1]
[1]*Department of Cell Biology and Anatomy,*
[2]*Interdepartmental Neuroscience Program,*
Rosalind Franklin University of Medicine and Science, North Chicago, IL
USA

1. Introduction

Invertebrate preparations have proven to be valuable models for studies addressing fundamental mechanisms of nervous system function (Clarac and Pearlstein 2007). In general the nervous systems of invertebrates contain fewer neurons than those of vertebrates, with many of them being re-identifiable in the sense that they can be recognized and studied in any individual of the species. The large diameter of many invertebrate neurons makes them amenable for study with intracellular recording techniques, allowing for characterization of synaptic properties and connections, leading to circuit diagrams of neuronal networks. Further, there is often a rather straight-forward connection between neuronal networks and the relatively simple behaviors that they produce. For example, years of experimentation on the nervous systems of leeches, sea-slugs and crabs/lobsters have led to significant advances in the understanding of how small neuronal networks produce a variety of different behaviors (Harris-Warrick and Marder 1991; Hawkins et al. 1993; Katz 1998; Kristan et al. 2005). For the most part, these investigations have been carried out using sharp electrode recordings from about three to four neurons at a time (although see (Briggman and Kristan 2006)). Intracellular recording has been a very productive and fruitful technique for revealing details of neuronal connectivity and for studying synaptic changes caused by modulators or by simple forms of learning. However, since even simple behaviors are produced by the activity of populations of dozens to hundreds of neurons, the limited view offered by recording from only four neurons at a time makes it an inadequate technique for understanding larger-scale, network level phenomena that underlie behavior.

In order to understand how populations of neurons produce behaviors, methods are needed to simultaneously monitor the spiking activity of large numbers (dozens to hundreds) of individual neurons. Voltage-sensitive dye (VSD) imaging is a technique for accomplishing precisely this. However, after a promising start showing the immense power and potential of VSD imaging for understanding invertebrate neuronal networks (London et al. 1987; Wu et al. 1994a; Wu et al. 1994b; Zecevic et al. 1989), the technique has not been widely adopted by the field. This is possibly due to the difficulties inherent to the technique - the optical signals of interest are extremely small and are often mixed, redundant and noisy. These factors make it difficult to track the activity of individual neurons from recording trial to trial based solely on the raw optical data. Previous researchers used a spike-template

matching technique to uncover single neuron spiking traces from VSD imaging data, but this method was very time consuming and involved substantial human judgment (Cohen et al. 1989). Automated, accurate and fast methods are thus needed to reliably and quickly extract single neuron spiking activity from such complex data sets.

In this chapter, we demonstrate the utility and accuracy of Infomax ICA for extracting single neuron spiking activity (i.e. spike-sorting) from VSD imaging data of populations of neurons located in the central ganglia of two invertebrate preparations, *Tritonia diomedea* and *Aplysia californica*, that are models for topics such as learning, modulation, pattern generation and pre-pulse inhibition (Brown et al. 2001; Cleary et al. 1998; Frost et al. 1998; Frost et al. 2006; Frost et al. 2003; Getting 1981; Katz and Frost 1995; Katz et al. 1994; Lennard et al. 1980). We also demonstrate certain features of the optical data sets that strongly influence the ability of ICA to return maximal numbers of components that represent the spiking activity of individual neurons (neuronal independent components or nICs).

2. Methods

2.1 Preparation

Tritonia diomedea central ganglia consisting of the bilaterally symmetric cerebral, pleural and pedal ganglia, and *Aplysia californica* central ganglia consisting of the cerebral, pleural and pedal ganglia, were dissected out and pinned onto the bottom of a Sylgard (Dow Corning) lined Petri dish containing Instant Ocean artificial seawater (Aquarium Systems). The thick connective tissue covering the ganglia and nerves was removed with fine forceps and scissors (for intracellular recording experiments the thin protective sheath covering the neurons was also removed). The preparation was then transferred and pinned to the Sylgard-lined coverslip bottom of the recording chamber used for optical recording (PC-H perfusion chamber, Siskiyou). In many experiments, to increase the number of neurons in focus, the ganglion to be imaged was flattened somewhat by pressing a cover slip fragment down upon it that was held in place with small blobs of Vaseline placed on the recording chamber floor.

2.2 Optical recording

Imaging was performed with an Olympus BX51WI microscope equipped with either 10x 0.6NA or 20x 0.95NA water immersion objectives. Preparation temperature was maintained at 10 – 11°C for *Tritonia* and 16 – 17°C for *Aplysia*, using Instant Ocean passed through a feedback-controlled in-line Peltier cooling system (Model SC-20, Warner Instruments). Temperature was monitored with a BAT-12 thermometer fitted with an IT-18 microprobe (Physitemp, Inc) positioned near the ganglion being imaged. For staining, the room was darkened and the perfusion saline was switched to saline containing the fast voltage sensitive absorbance dye RH-155 (Anaspec). Staining was carried out in one of two ways: either 5 min of 0.3 mg/ml or 1.5 hr of 0.03 mg/ml RH-155 in saline. Preparations were then perfused with 0.03 mg/ml RH-155 or dye-free saline throughout the experiment. Trans-illumination was provided with light from a 100W tungsten halogen lamphouse that was first passed through an electronic shutter (Model VS35 Vincent Associates), a 725/25 bandpass filter (Chroma Technology), and a 0.9 NA flip top achromat Nikon condenser on its way to the preparation. 100% of the light from the objective was directed either to an Optronics Microfire digital camera used for focusing and to obtain an image of the preparation to superimpose with the imaging data, or to the parfocal focusing surface of a 464-element photodiode array (NeuroPDA-III, RedShirtImaging) sampled at 1600 Hz.

2.3 Sharp electrode recordings

Intracellular recordings were obtained with 15-30 MΩ electrodes filled with 3M KCl or 3M K-acetate connected to a Dagan IX2-700 dual intracellular amplifier. The resulting signals were digitized at 2 KHz with a BioPac MP 150 data acquisition system.

2.4 Data analysis

Optical data were bandpass filtered in the Neuroplex software (5 Hz high pass and 100 Hz low pass Butterworth filters; RedShirtImaging), and then processed with ICA in MATLAB to yield single neuron action potential traces (independent components), see (Hill et al. 2010) for details. ICA run on 60 s of optical data typically takes about 5 minutes on a computer equipped with an Intel I7 processor. Statisical analyses were performed in Sigmaplot.

3. Results

We bath applied the VSD RH-155 to the central ganglia of *Tritonia diomedea* and *Aplysia californica*, and used a 464-element photodiode array to image the action potential activity of populations of neurons on the surface of various ganglia during two rhythmic motor programs: escape swimming in *T. diomedea*, and escape crawling in *A. californica*. Here we show examples of ICA's ability to extract single neuron activity from mixed, redundant and noisy raw optical data in both *T. diomedea* **(Fig. 1)** and *A. californica* **(Fig. 2)** and we demonstrate the ability of ICA to return maps of the neurons' locations in the ganglia (based on the inverse weight matrix).

3.1 Validation of the accuracy of ICA

We previously demonstrated the accuracy of ICA spike-sorting by performing simultaneous intracellular and optical recordings in both *Tritonia* and *Aplysia* (Hill et al. 2010): in 34 out of 34 cases, one of the independent components returned by ICA matched up perfectly spike-for-spike with the intracellularly recorded data. **Figure 3** shows an intracellular recording from a *Tritonia* pedal ganglion neuron while simultaneously recording the optical activity of many neurons in the same ganglion. The activity of the intracellularly recorded neuron was detected by many diodes (**Fig. 3Ai**). ICA returned 50 nICs, one of which matched up perfectly spike-for-spike with the intracellularly recorded neuron **(Fig. 3Aii, iii and 3B)**. Plotting the data points for the intracellular and matching component traces against each other reveals a strong positive correlation (**Fig. 3C**; R^2 value = 0.631). Another of the nICs burst in the same phase of the swim motor program as did the intracellularly recorded neuron (**Fig. 3D**), however plotting the values of the intracellular and non-matching component against each other revealed no correlation whatsoever (**Fig. 3E**). **Figure 4** shows an intracellular recording from an *Aplysia* buccal ganglion neuron while simultaneously recording the optical activity of many neurons in the same ganglion. The activity of the intracellularly recorded neuron was detected by many diodes (**Fig. 4Ai**). ICA returned 10 nICs, one of which matched up perfectly spike-for-spike with the intracellularly recorded neuron **(Fig. 4Aii, iii and 4B)**. Plotting the data points for the intracellular and matching component traces against each other revealed a strong positive correlation (**Fig. 4C**; R^2 value = 0.629).

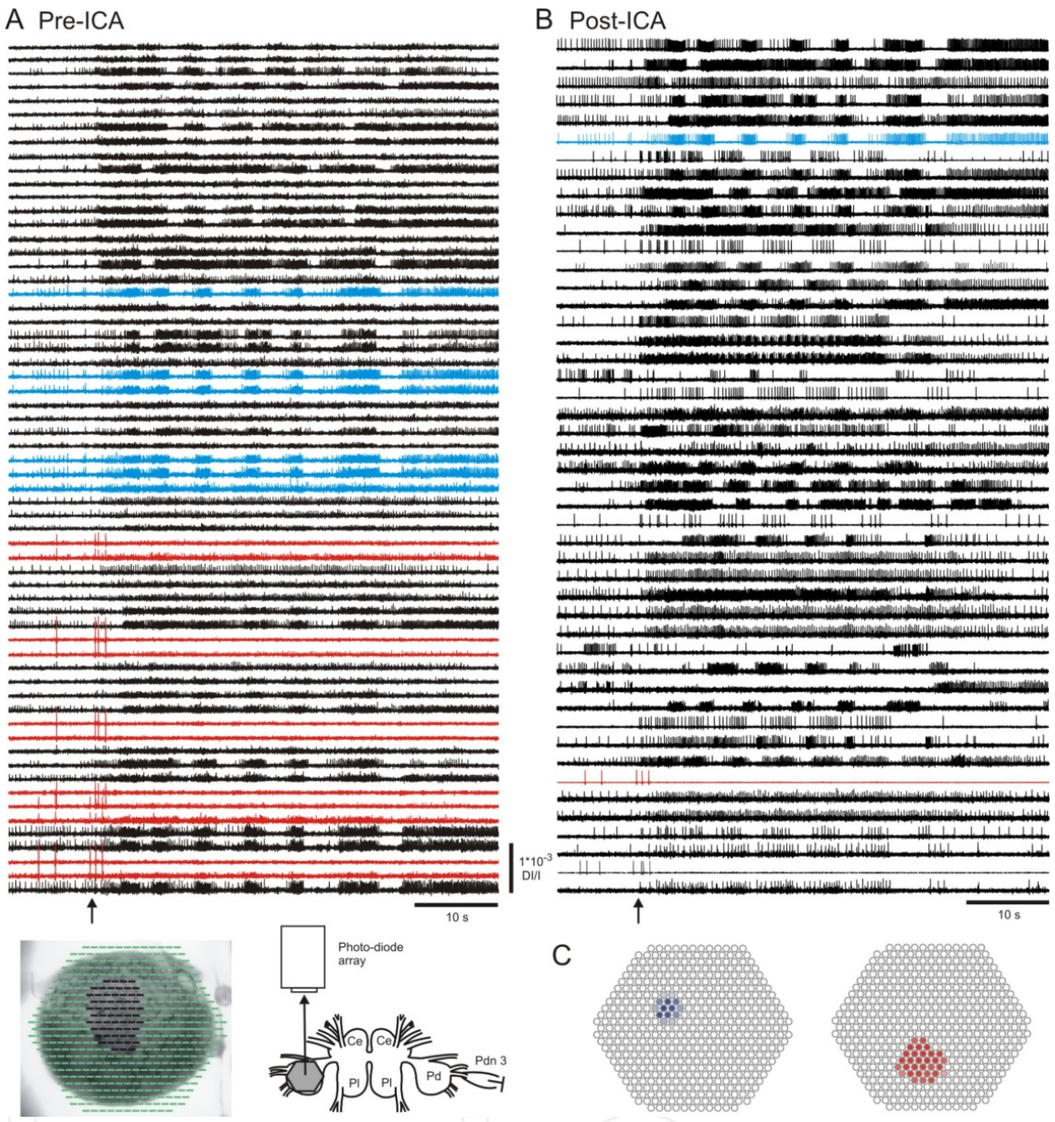

Fig. 1. ICA returns single neuron traces from noisy, redundant, and mixed raw optical data of a *Tritonia diomedea* swim motor program.
A The subset of diodes shown in black superimposed over an image of the pedal ganglion (inset) detected the spiking activity of many pedal ganglion neurons. The optical signals are redundant in the sense that many diodes detect the activity of the same neurons, and mixed in the sense that many diodes detect the activity of more than one neuron. Note that diode traces shown in blue redundantly detected the activity of the same neuron, as did the diode traces shown in red. Experimental set-up shown below the optical traces. Ce = cerebral, Pl = pleural, Pd = pedal ganglion, and pdn 3 = pedal nerve 3. **B** 123 of the 464 independent components returned by ICA represented the activity of single neurons (47 shown here). The redundancy of the optical data was eliminated by ICA – note that the blue and red independent components represent the activity of the two neurons that were detected by multiple diodes in **A**. **C** The maps returned by ICA show the ganglion locations of the neurons whose spiking activity is shown in blue and red in **A** and **B**. Arrows – stimulus to pedal nerve 3 to elicit swim motor program (10 V, 10 Hz, 2 s).

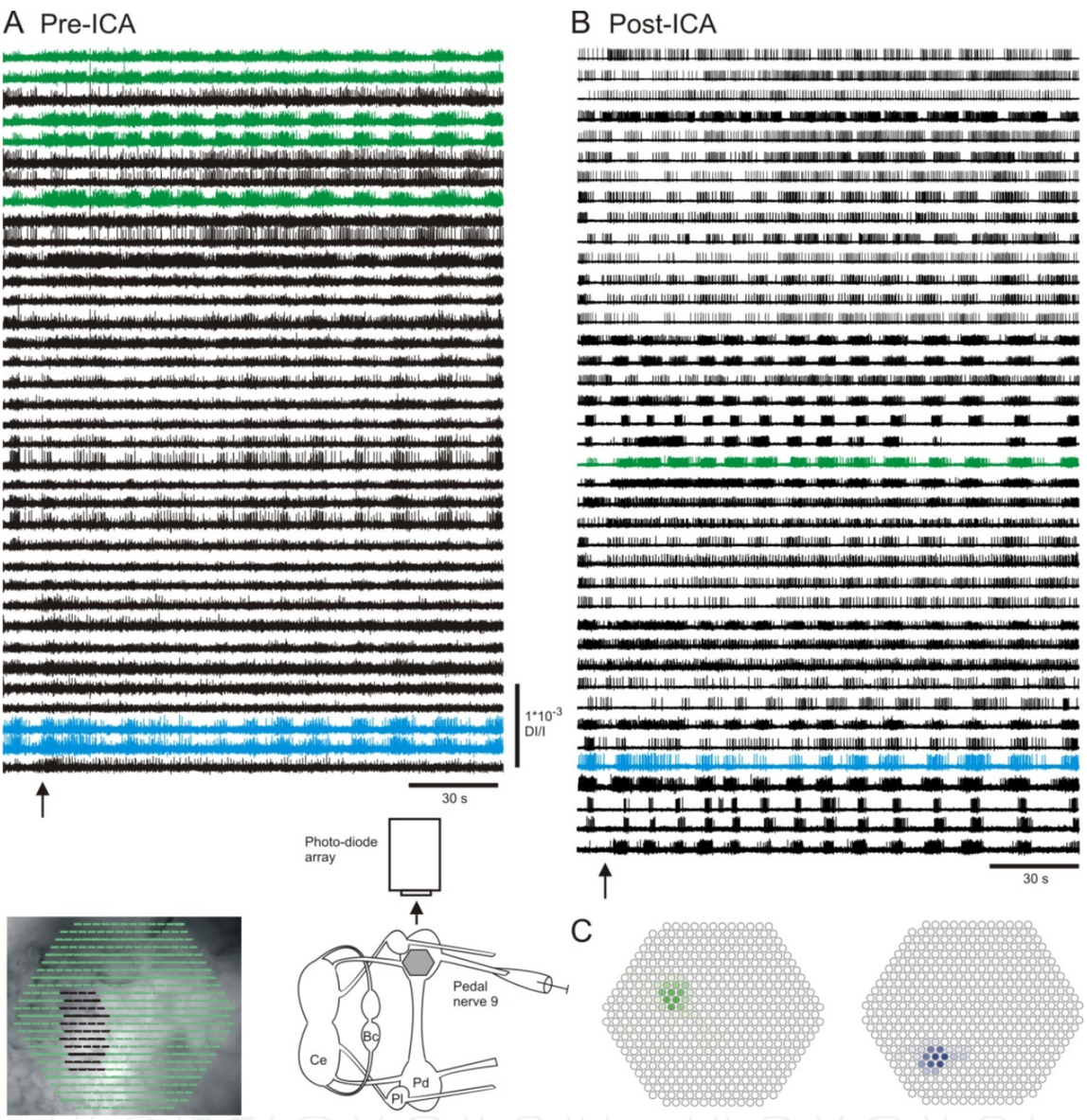

Fig. 2. ICA extracts the activity of individual pedal ganglion neurons from noisy, redundant, and mixed raw optical data of an *Aplysia californica* locomotion motor program.
A The neural activity of many pedal ganglion neurons was detected by a subset of the 464 diodes shown in black (inset, diode array superimposed over an image of the pedal ganglion). Note that diode traces shown in green detected the activity of the same neuron, as did the diode traces shown in blue. Experimental set-up showing the region of the pedal ganglion imaged shown in the inset. Bc = buccal, Ce = cerebral, Pl = pleural, and Pd = pedal ganglion. **B** 95 of the 464 independent components returned by ICA represented the activity of single neurons (45 shown here). Note that the redundancies shown in **A** were eliminated by ICA. **C** The maps returned by ICA show the ganglion locations of the neurons whose spiking activity is shown in green and blue in **A** and **B**. Arrows – stimulus to pedal nerve 9 to elicit the locomotion motor program (10 V, 1 Hz, 155 s).

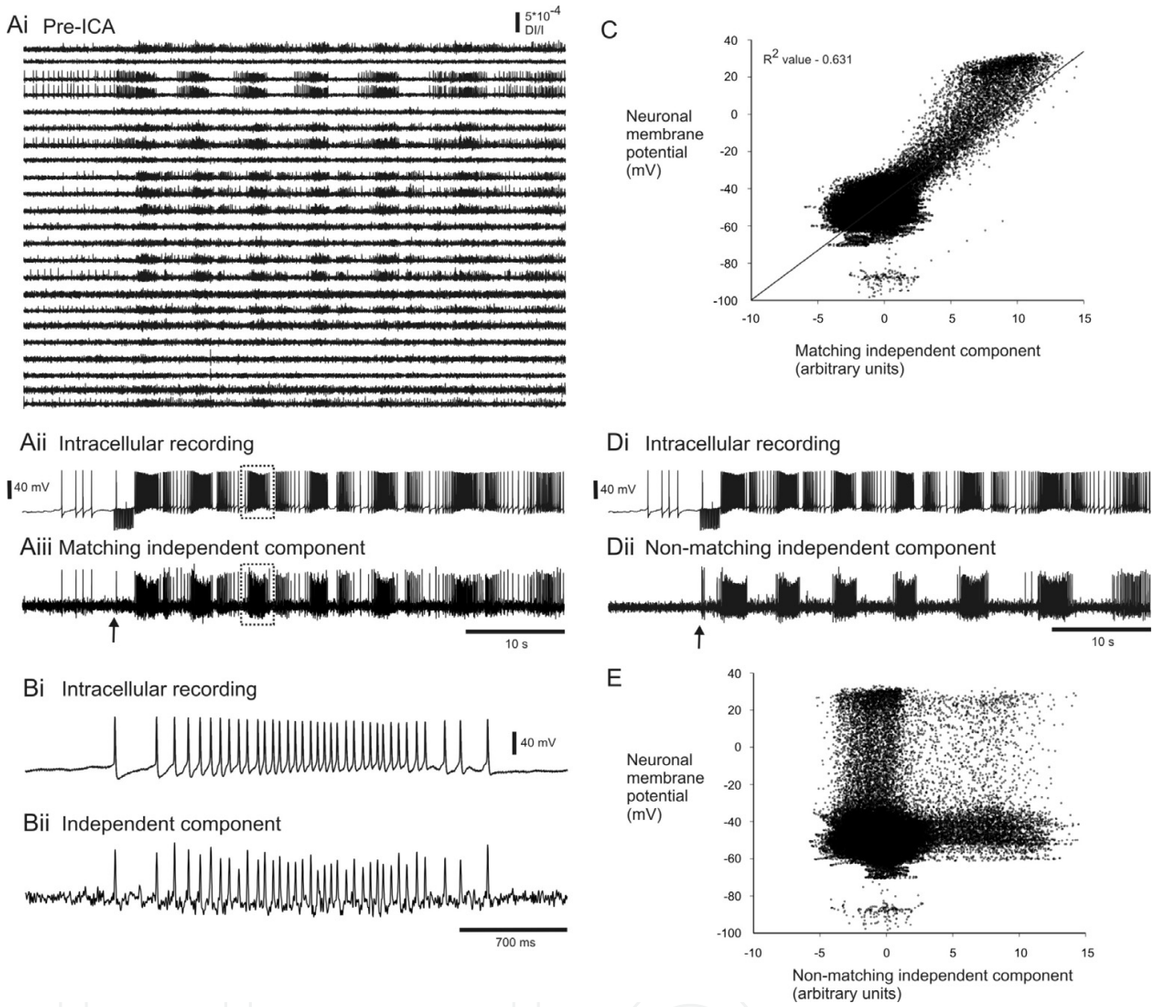

Fig. 3. Validation of the accuracy of ICA in *Tritonia diomedea.*
A Simultaneous intracellular recording from a pedal ganglion neuron and VSD imaging from the same ganglion of *T. diomedea* during a swim motor program. **Ai** Many of the diode traces contained the spiking of activity of the intracellularly recorded neuron. **Aii, Aiii** After performing ICA on the entire data set (464 filtered optical traces), one of the independent components returned by ICA matched up exactly spike-for-spike with the intracellular trace. **B** Expanded view of the traces shown in **Aii** and **Aiii** (dashed boxes). **C** Plotting the values of the intracellular recording trace versus the matching component revealed a positive correlation between the data points. **D** Another of the components returned by ICA appeared similar to the intracellular recording trace in that it burst in the same phase of the motor program. **E** Plotting the values of the intracellular recording trace versus the non-matching component showed no correlation at all between the data points. Arrows – stimulus to pedal nerve 3 (10v, 10 Hz, 2 s).

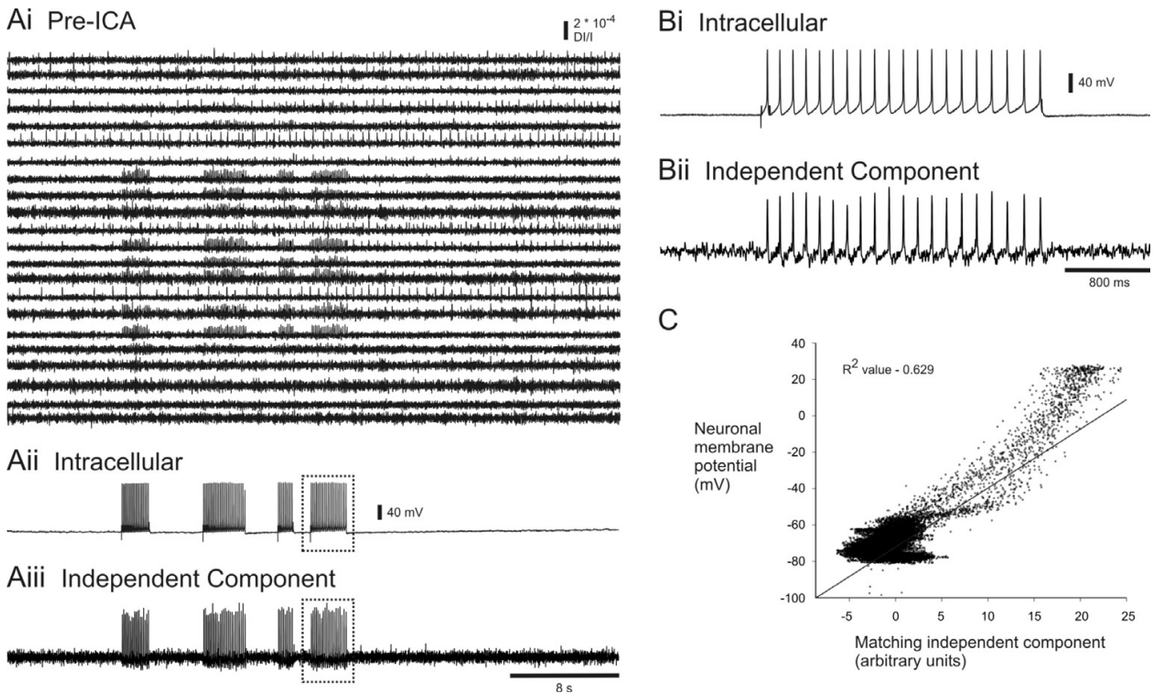

Fig. 4. Validation of the accuracy of ICA in *Aplysia californica.*
A Simultaneous intracellular recording from a buccal ganglion neuron and VSD imaging from the same ganglion of *A. californica*. Current pulses were injected into the impaled neuron to make it to fire trains of action potentials. **Ai** Many of the diode traces contained the spiking of activity of the intracellularly recorded neuron. **Aii, Aiii** After running ICA on the entire data set, one of the independent components returned by ICA matched up exactly spike-for-spike with the intracellular trace. **B** Expanded view of the traces shown in **Aii** and **Aiii** (dashed boxes). **C** Plotting the values of the intracellular recording trace versus the matching component revealed a positive correlation between the data points.

3.2 Certain features of the data sets influence the number of nICs returned by ICA

Next we discuss our findings that certain features of the optical data sets strongly influence the number of nICs returned by ICA. First, we found that simply increasing the number of data points in the optical recording greatly increases the number of nICs returned by ICA (**Fig. 5A**). This could be due to the fact that with longer files, ICA is simply given more information, and is thus better able to determine which components are independent of each other. Increasing the file length only continues to increase the number of nICs returned by ICA up to a certain point though, usually around 45 s (for our data sets). Increasing file length also greatly decreases the variability of the number of nICs returned by ICA **(Fig. 5A)**. We have also found that including spontaneous spiking activity (at least 10 s) preceding the *Tritonia* escape swim motor program greatly increases the number of nICs returned by ICA (**Fig. 5B, C**). For example, for seven preparations we found that when ICA was performed on 40 s of optical data including 10 s of spontaneous firing data preceding the swim motor program it returned a mean of 68.8 nICs, while ICA returned a mean of only 44.5 nICs when it was run on 40 s optical files that didn't include any spontaneous

firing preceding the motor program **(Fig. 5C)**. Presumably neurons are more independent of each other when they are firing spontaneously than when they are bursting in near synchrony during the swim motor program. Thus, this period of greater independence is important for ICA to return maximal numbers of nICs.

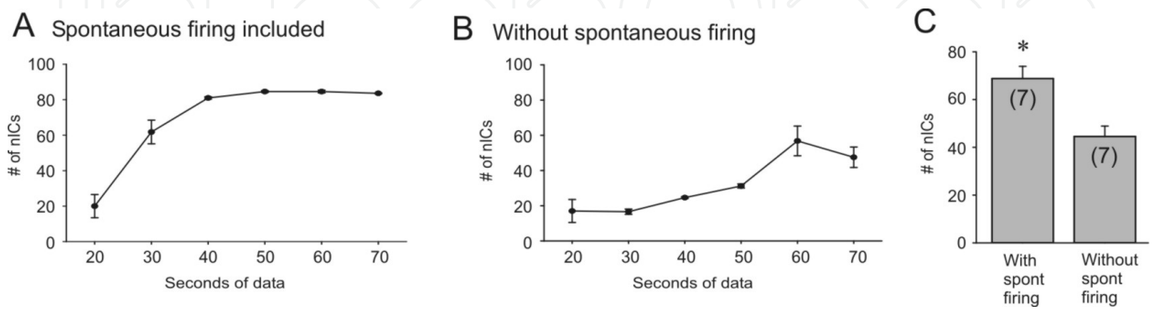

Fig. 5. Increasing file length and including spontaneous firing data improve the performance of ICA.
A Increasing file length leads to an increase in the number of nICs returned by ICA. The points on the graph show the average number of nICs returned by ICA for each data length. Note that with the shorter data lengths there is a fairly large variance in the number of nICs returned by ICA run on the exact same data set. This variance decreases greatly with increasing file length. After a certain point (~ 45 s) having more data points didn't increase the number of nICs returned by ICA. **B** Including spontaneous spiking data preceding the rhythmic swim motor program data is important for ICA to return a maximal number of nICs. The points on the graph show the average number of nICs returned by ICA for each data length. Without the spontaneous firing data (10 s) included before the swim motor program, ICA returned fewer nICs even with longer files (same data set as in **A**). **C** In seven preparations, including 10 s of spontaneous firing data preceding the swim motor program significantly increased the average number of nICs returned by ICA for optical files of equal length (With spont firing = 10 s spontaneous firing + 30 s motor program, Without spont firing = 40 s motor program; paired t-test, * = $p < 0.05$).

3.3 Pre-filtering the data also strongly influences the number of nICs returned by ICA

Finally, we have found that filtering the optical data prior to running ICA to remove high frequency (100 Hz LP) and low frequency noise (5 Hz HP) consistently increases the number of nICs returned by ICA, and increases the signal-to-noise ratio of the nICs. **Figure 6** shows an example of the effect of pre-filtering on the number of nICs returned by ICA. Without pre-filtering, ICA returned 34 nICs (**Fig. 6A**) whereas after pre-filtering it returned 73 nICs (**Fig. 6B**). Removing the low frequency noise in particular should make the components more independent of each other.

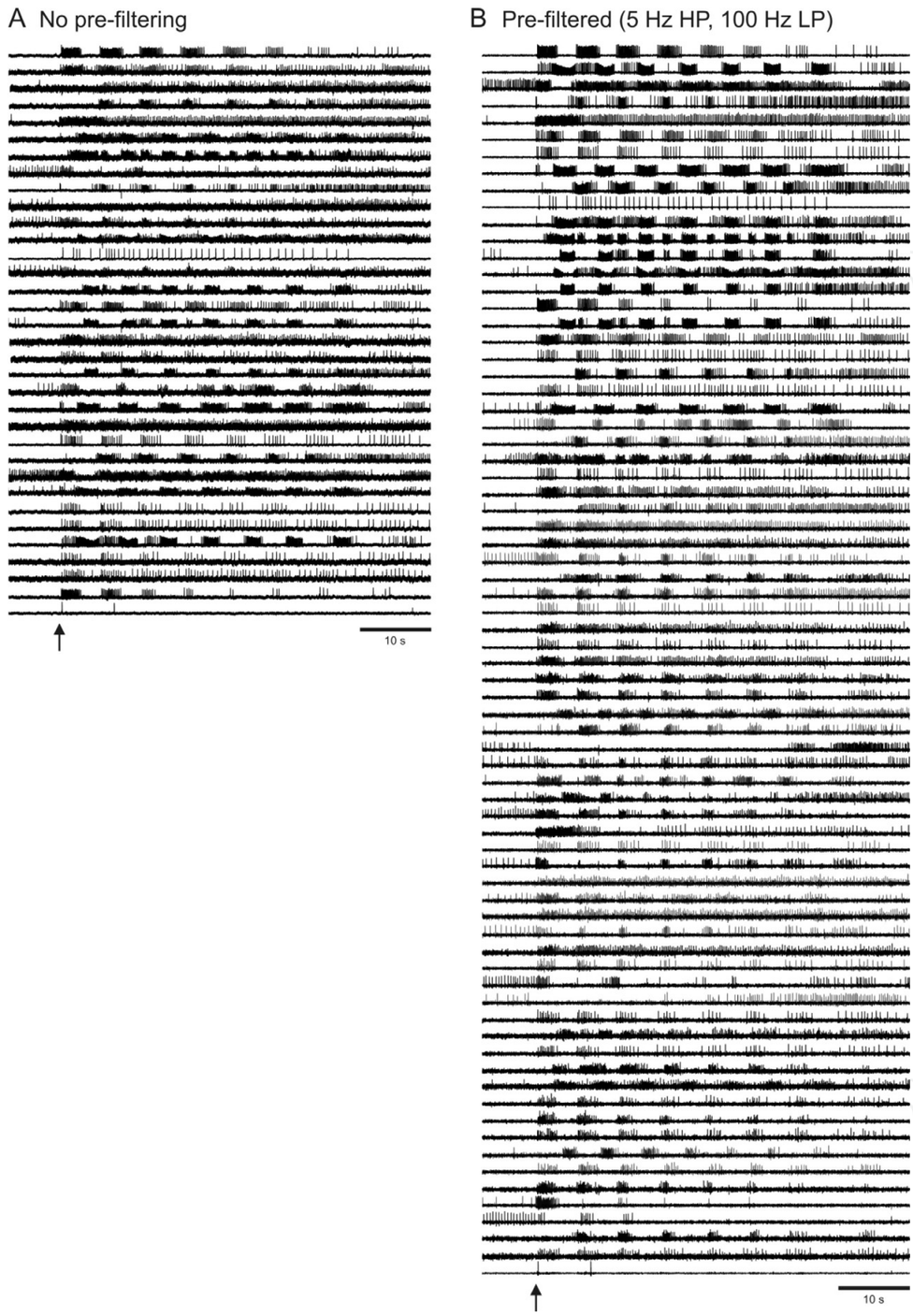

Fig. 6. Pre-filtering the optical data prior to performing ICA increases the number of nICs returned.
A ICA run on unfiltered optical data returned 34 nICs. **B** After pre-filtering the same data set (5 Hz HP, 100 Hz LP), ICA returned 73 nICs. Additionally pre-filtering the optical data increased the signal-to-noise ratio of the nICs. Arrows – stimulus to pedal nerve 3 (10 V, 10 Hz, 2 s).

4. Conclusions

ICA is an ideal technique for quickly and accurately extracting single neuron spiking activity from noisy, mixed and redundant VSD imaging data. The lack of a technique such as ICA has possibly hindered widespread use of fast VSD imaging as a tool to study invertebrate neuronal networks. Here we have shown examples of ICA's ability to extract single neuron spiking activity from optical files of escape motor programs in *Tritonia* and *Aplysia*. Additionally, we have demonstrated the accuracy of ICA with simultaneous intracellular and optical recording in the two molluscan species. We have also demonstrated that features of the optical data sets such as file length and the inclusion of spontaneous firing data are important for ICA to return a maximal number of components that represent the activity of individual neurons. Finally, we have shown that pre-filtering the optical data to remove high and low frequency noise is also beneficial for ICA to return maximal numbers of components that represent the activity of individual neurons.

5. Future directions

The combination of fast VSD imaging and ICA may lead to a resurgence in the use of fast VSDs for deciphering how invertebrate neuronal networks operate and are modified with experience. While the combination of VSD imaging and ICA makes it possible to monitor the activity of well over one hundred neurons during various motor programs, methods are now needed to reveal how sub-groups or ensembles of neurons within these datasets behave during the production of various behaviors. Fortunately, many researchers have developed methods that do precisely this. For example, a recently developed spike-train correlation analysis method called the Functional Clustering Algorithm (Feldt et al. 2009) reveals clusters of neurons that fire spikes together in a statistically significant manner. Using the FCA, we have examined how functional clusters of neurons in the *Tritonia* pedal ganglion change with the transition from escape swimming to post-swim crawling (Hill et al. 2011). Finally, since ICA can be performed rapidly, during the course of an experiment, it will be possible to identify neurons of interest and then to impale those neurons with sharp electrodes and determine their roles in network function.

6. Acknowledgments

The authors thank Caroline Moore-Kochlacs and Terry Sejnowski for helping us implement ICA and Jean Wang for technical assistance with some of the optical recordings.

7. References

Briggman KL, and Kristan WB, Jr. Imaging dedicated and multifunctional neural circuits generating distinct behaviors. *J Neurosci* 26: 10925-10933, 2006.

Brown GD, Yamada S, and Sejnowski TJ. Independent component analysis at the neural cocktail party. *Trends in neurosciences* 24: 54-63, 2001.

Clarac F, and Pearlstein E. Invertebrate preparations and their contribution to neurobiology in the second half of the 20th century. *Brain research reviews* 54: 113-161, 2007.

Cleary LJ, Lee WL, and Byrne JH. Cellular correlates of long-term sensitization in Aplysia. *J Neurosci* 18: 5988-5998, 1998.

Cohen L, Hopp HP, Wu JY, Xiao C, and London J. Optical measurement of action potential activity in invertebrate ganglia. *Annu Rev Physiol* 51: 527-541, 1989.

Feldt S, Waddell J, Hetrick VL, Berke JD, and Zochowski M. Functional clustering algorithm for the analysis of dynamic network data. *Physical review* 79: 056104, 2009.

Frost WN, Brandon CL, and Mongeluzi DL. Sensitization of the Tritonia escape swim. *Neurobiology of learning and memory* 69: 126-135, 1998.

Frost WN, Brandon CL, and Van Zyl C. Long-term habituation in the marine mollusc Tritonia diomedea. *The Biological bulletin* 210: 230-237, 2006.

Frost WN, Tian LM, Hoppe TA, Mongeluzi DL, and Wang J. A cellular mechanism for prepulse inhibition. *Neuron* 40: 991-1001, 2003.

Getting PA. Mechanisms of pattern generation underlying swimming in Tritonia. I. Neuronal network formed by monosynaptic connections. *Journal of neurophysiology* 46: 65-79, 1981.

Harris-Warrick RM, and Marder E. Modulation of neural networks for behavior. *Annual review of neuroscience* 14: 39-57, 1991.

Hawkins RD, Kandel ER, and Siegelbaum SA. Learning to modulate transmitter release: themes and variations in synaptic plasticity. *Annual review of neuroscience* 16: 625-665, 1993.

Hill ES, Moore-Kochlacs C, Vasireddi SK, Sejnowski TJ, and Frost WN. Validation of independent component analysis for rapid spike sorting of optical recording data. *Journal of neurophysiology* 104: 3721-3731, 2010.

Hill ES, Vasireddi S, Wang J, Maruyama D, Zochowski M, and Frost WN. A method for monitoring the temporal structure of neuronal networks. In: *Society for Neuroscience Annual Meeting*. Washington, D.C.: 2011.

Katz PS. Neuromodulation intrinsic to the central pattern generator for escape swimming in Tritonia. *Annals of the New York Academy of Sciences* 860: 181-188, 1998.

Katz PS, and Frost WN. Intrinsic neuromodulation in the Tritonia swim CPG: the serotonergic dorsal swim interneurons act presynaptically to enhance transmitter release from interneuron C2. *J Neurosci* 15: 6035-6045, 1995.

Katz PS, Getting PA, and Frost WN. Dynamic neuromodulation of synaptic strength intrinsic to a central pattern generator circuit. *Nature* 367: 729-731, 1994.

Kristan WB, Jr., Calabrese RL, and Friesen WO. Neuronal control of leech behavior. *Progress in neurobiology* 76: 279-327, 2005.

Lennard PR, Getting PA, and Hume RI. Central pattern generator mediating swimming in Tritonia. II. Initiation, maintenance, and termination. *Journal of neurophysiology* 44: 165-173, 1980.

London JA, Zecevic D, and Cohen LB. Simultaneous optical recording of activity from many neurons during feeding in Navanax. *J Neurosci* 7: 649-661, 1987.

Wu JY, Cohen LB, and Falk CX. Neuronal activity during different behaviors in Aplysia: a distributed organization? *Science* 263: 820-823, 1994a.

Wu JY, Tsau Y, Hopp HP, Cohen LB, Tang AC, and Falk CX. Consistency in nervous systems: trial-to-trial and animal-to-animal variations in the responses to repeated applications of a sensory stimulus in Aplysia. *J Neurosci* 14: 1366-1384, 1994b.

Zecevic D, Wu JY, Cohen LB, London JA, Hopp HP, and Falk CX. Hundreds of neurons in the Aplysia abdominal ganglion are active during the gill-withdrawal reflex. *J Neurosci* 9: 3681-3689, 1989.

IntechOpen

IntechOpen

© 2012 The Author(s). Licensee IntechOpen. This is an open access article distributed under the terms of the Creative Commons Attribution 3.0 License, which permits unrestricted use, distribution, and reproduction in any medium, provided the original work is properly cited.

IntechOpen

IntechOpen